Multiple Active Site Monte Carlo Model for Heterogeneous Ziegler-Natta Propylene Polymerization

Zheng-Hong Luo, De-Pan Shi, Yong Zhu

Department of Chemical and Biochemical Engineering, College of Chemistry and Chemical Engineering, Xiamen University, Xiamen 361005, People's Republic of China

Received 9 May 2009; accepted 3 September 2009
DOI 10.1002/app.31388
Published online 26 October 2009 in Wiley InterScience (www.interscience.wiley.com).

ABSTRACT: In this study, the kinetics of propylene polymerization catalyzed with the fourth heterogeneous Ziegler-Natta catalyst is studied. More than one type of active site is present in the propylene polymerization based on an analysis of the GPC curves. A multiple active site kinetic model (MSmodel) is proposed by using Monte Carlo technique. Good agreements in the polymerization kinetics are achieved for fitting the kinetic profiles with the MSmodel. In addition, the MSmodel is used to describe the dynamic evolutions of the active sites and their effects on the propylene polymerization. The simulated results indicate that different types of active sites have different polymerization kinetics and the site type can affect the propylene polymerization kinetics. © 2009 Wiley Periodicals, Inc. J Appl Polym Sci 115: 2962–2970, 2010

Key words: propylene polymerization; heterogeneous Ziegler-Natta catalyst; multiple active site; kinetic model; Monte Carlo technique

INTRODUCTION

Polymerization kinetics is always an important proportion of polymerization engineering, which describes the changes of polymerization activity and polymer properties dependent on polymerization time.[1,2] In addition, the polymerization kinetics can be described using model equations. There are two leading modeling methods, namely, statistic modeling method and mechanism modeling method.[2,3] Recently, Monte Carlo technique has been introduced and received many attentions in the field of polymerization kinetics with the development of computer technique and mathematical algorithm.[4–8] The ability of the Monte Carlo technique to model the complete polymerization process or even product properties facilitates a more rigorous examination of whether the assumed kinetic mechanism and coefficients provide an adequate representation of the polymerization itself.[4]

Up to now, there have been many published articles[1,2,9–12] regarding the polymerization kinetics. However, past studies from microscale level are not common. The studies on the microscale polymerization kinetics based on the Monte Carlo technique are even less.

On the other hand, in the polymerization field, propylene polymerization has attracted lots of attentions owing to the simple configuration and various applications of polypropylene (PP) produced via the propylene polymerization. For the propylene polymerization kinetics, most of published articles are concerned with the heat and mass transfer behaviors inside the catalyst particles from mesoscale level.[2,13–16] Recently, Luo et al.[12,17] proposed a novel kinetic scheme and studied the effects of polymerization temperature and impurity etc. on the propylene polymerization kinetics by the Monte Carlo method. Luo et al.' model provided certain valuable information about the polymerization kinetics from macroscale level. In addition, Luo et al.[12,17] considered the heterogeneous Ziegler-Natta catalyst as a homogeneous catalyst, namely single active site type catalyst. Luo et al.[18] also investigated the effects of the elementary kinetic mechanism on the propylene polymerization by using the Monte Carlo method, but no any actual datum was given and the kinetic controlling mechanism was not studied. Simon et al.[19] developed a dynamic Monte Carlo model to describe the chain length distribution of polyolefins made with coordination catalysts dependent on the polymerization time. Their model displayed favorable flexibility compared with the GPC curves obtained from experiments, but no any microscale kinetic datum of the active site type was given. In addition, Simon et al.[20] also studied the copolymerization kinetics of ethylene and α-olefins by the Monte

Correspondence to: Z.-H. Luo (luozh@xmu.edu.cn).
Contract grant sponsor: National Natural Science Foundation of China; contract grant number: 20406016.
Contract grant sponsor: Fujian Petrochemical Company of SINOPEC.

Carlo method. Although particular emphasis has been given on the unique branch distribution of the copolymer, the microscale kinetics of the active site type has not been well studied.

Based on the previous discussion, it is clear that most of past models of olefin polymerization proposed using the Monte Carlo method suppose that there exists single-active site type in the polymerization system. It is also clear that there is a lack of literatures about the microscale kinetics of active site type in the propylene polymerization field. In practice, the conclusions that there exists multiple active site types in the propylene polymerization process catalyzed with Ziegler-Natta catalysts or Phillips catalysts have been proved.[21,22] Therefore, it is necessary to study the microscale kinetics of the propylene polymerization system including multiple active site types. In this study, the propylene polymerization kinetics catalyzed with the fourth heterogeneous Ziegler-Natta catalyst is studied. Five types of active sites are present in the polymerization based on an analysis of the GPC curves. A multiple active site kinetic model (MSmodel) is proposed by using the Monte Carlo technique. Particular attention is paid to describe the dynamic evolutions of the active sites and their effects on the polymerization kinetics by using the Monte Carlo technique. Furthermore, the MSmodel data are compared with the experimental data.

EXPERIMENTAL

Materials

Nitrogen and polymerization-grade propylene (Sinopec, China) were purified by passing through CuO catalyst, and 4 Å molecular sieves. The catalyst system used in this study was a commercially available Ziegler-Natta catalyst defined the fourth generation CS-1 catalyst (Xiangyang, China), with $TiCl_4$ on a $MgCl_4$ support. Triethylaluminum (Lanzhou Petrochemical Company Research Institute, China) was used as cocatalyst and di-cyclopentyldimmethoxy silane (Lanzhou Petrochemical Company Research Institute, China) was used as external electron donor.

Polymerization procedure

All manipulations involving air and moisture sensitive compounds were performed using a standard Schlenk technique. All polymerizations were performed in a 100 mL glass autoclave equipped with propylene inlet, magnetic stirrer,vacuum line press control device and temperature control device. The autoclave was firstly filled with 50 mL dry hexane and certain quantities of the CS-1 PP catalyst (CS-1 catalyst), triethylaluminum ($AlEt_3$) and di-cyclopentyldimmethoxy silane. Propylene was added into the autoclave via a magnetic valve. Polymerizations were carried out at 40°C for certain time and terminated by acidified ethanol. The press in the autoclave during the polymerizations was controlled at 0.02 MPa via the press control device. The resulting polymer was separated by filtration and dried under vacuum until constant weight. To obtain the bulk polymerization kinetics based on polymerization experiment, the mass transfer limitation should be eliminated. Based on our preliminary experiments, we found that the polymer yield-time curves are identic when the stirring speed is 1500 rpm or more (here no experimental results are given). Namely, the stirring speed was 1500 rpm, at which the diffusion effect on the polymerizations was minimized and could be ignored.[23–25]

Measurement

High temperature GPC was performed with a Alliance GPC-V2000 instrument at at 135°C using 1,2-dichlorobenzene as the solvent. In addition, the polymer yield was continuously recorded by magnetic valve as a function of time and the polymerization rate was obtained by further differentiation.

MODEL DEVELOPMENT

Propylene polymerization mechanism

To describe the propylene polymerization kinetics on the CS-1 catalyst, a simple kinetic model is invoked.[11,12,17,26–28] The polymerization kinetic scheme comprises a series of elementary reactions, namely, chain initiation, chain propagation, chain transfer and chain termination reactions. In addition, the following kinetic modeling assumptions are made in this article:

1. The same series of elementary reactions occur on any active site,
2. Only chain transfer to monomer is considered,
3. The value of the rate constant for each step is independent on the chain length,
4. For each active site, the value of the chain initiation rate constant is equal to that of the chain propagation rate constant.

Therefore, for the jth active site ($j = 1,2,\ldots$), the following elementary reactions can be obtained:

$$\text{Chain initiation:} \quad C_j^* + M \xrightarrow{k_{i,j}} P_{1,j}^*, \tag{1}$$

$$\text{Chain propagation:} \quad P_{r,j}^* + M \xrightarrow{k_{p,j}} P_{r+1,j}^*, \tag{2}$$

Chain transfer to monomer:

$$P^*_{r,j} + M \xrightarrow{k_{\mathrm{trm},j}} P^*_{1,j} + D_{r,j}, \quad (3)$$

$$\text{Chain termination:} \quad P^*_{r,j} \xrightarrow{k_{d,j}} D_{r,j}, \quad (4)$$

where, C^*_j represents the jth active catalyst site; M represents propylene; $P^*_{r,j}$ represents the active chains of length r ($r = 1,2,3,\ldots$) for the jth active site; $D_{r,j}$ represents the PP of chain length r ($r = 1,2,3,\ldots$) for the jth active site; $k_{i,j}$ represents the propylene initiation rate constant for the jth active site, L/mol s; $k_{p,j}$ represents the chain propagation rate constant for the jth active site, which value is equal to that of $k_{i,j}$ L/mol s; $k_{\mathrm{trm},j}$ represents the rate constant of chain transfer to propylene for the jth active site, L/mol s; $k_{d,j}$ represents the chain termination rate constant for the jth active site, s^{-1}. In addition, the number of the active site types of the CS-1 catalyst is obtained via the deconvolution of molecular weight distribution (MWD) described in the following section.[29]

Deconvolution of MWD data

To develop the MSmodel, the number of the active site types of the CS-1 catalyst must be obtained firstly. A simple approach was developed by Kissin,[29] which provides a means to extract detailed MWD information from GPC data.

Many polymerization kinetic experiments at different polymerization conditions, including temperature, catalyst mass, atomic ratio of Si/Al, etc., are accomplished. Corresponding GPC curves/data are obtained. However, the results obtained by extracting MWD information from the GPC curves according to Kission' approach[29] are similar. In our previous work,[25] we recorded the polymerization kinetic data under the same experimental conditions as those in this work except the atomic ratio of Si/Al. In practice, Kission' s approach is the resolution of GPC curves using the Flory distribution equation.[29]

This algorithm assumed that each site type produces a most-probable MWD,

$$w_i(n) = \tau_i{}^2 n \exp(-\tau_i n), \quad (5)$$

where $w_i(n)$ is the weight fraction of polymer of chain length n produced by each site type i and τ_i is the reverse of the number-average molecular weight of the polymer in site type i. And the chain-length distribution of the composite polymer is the sum of these distributions weighted by the mass fractions of polymer produced at each site type:

$$W(n) = \sum_{i=1}^{j} m_i w_i(n), \quad (6)$$

where $W(n)$ is the total weight fraction of polymer of chain length n; m_i is the mass fraction of polymer produced at each site type, and j is the total number of site types. During the deconvolution procedure, j pairs of m_i and τ_i are fitted simultaneously to match the GPC data of plant sample.

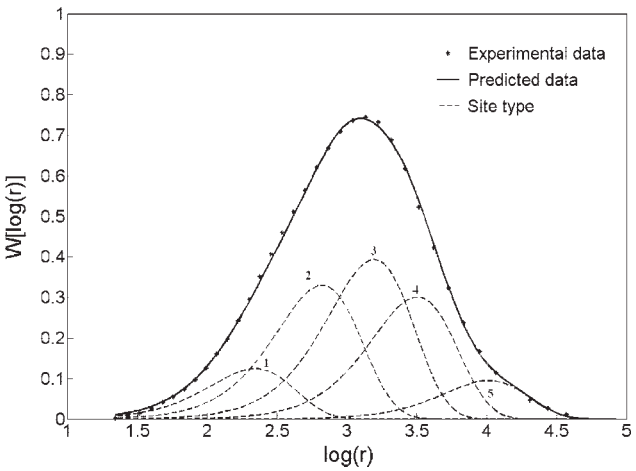

Figure 1 Resolution for GPC curves of PP produced by CS-1 catalyst. Experimental data at $T = 313$ K, Al/Ti = 98 (mol/mol), Si/Al = 0.05 (mol/mol), and $t = 1$ hr. r represents the chain length, and w represents the most probable chain-length distributions.

Accordingly, the experimental GPC curves of the polymers can be described by 4 and over Flory-distribution components with different molecular weights. Namely, the most-probable number of site types is found to be 4 or over. In addition, we also find that the errors between the fitting data obtained via Kission's approach[29] and the experimental data are almost equal at the most-probable number of 4 and over. Corresponding correlation coefficients for the experimental data are also almost equal. Therefore, considering the computational simplify in the following work, we choose five active site types for the CS-1 catalyst in this study. Here, two of the representative sets of the results are shown in Figures 1 and 2 and Table I to prove the value of the most probable number of site types. Corresponding discussion is performed later.

MS Monte Carlo model methodology

The principle of multiple active site (MS) Monte Carlo modeling for the propylene polymerization is based on Gillespie's algorithm.[30] In addition, as described in the introduction section, there are some published articles regarding the Monte Carlo modeling applied in polymerization field.[6,7,12,17–20,30,31] Therefore, here, we describe the fundamental principles of the Monte Carlo methodolgy briefly, which were reported in Refs. 6, 7, 12, 17–20, 30, 31. For a certain polymerization, when its elementary reactions are presumed or certain, the general operation mode of such a method is as follows. The reaction

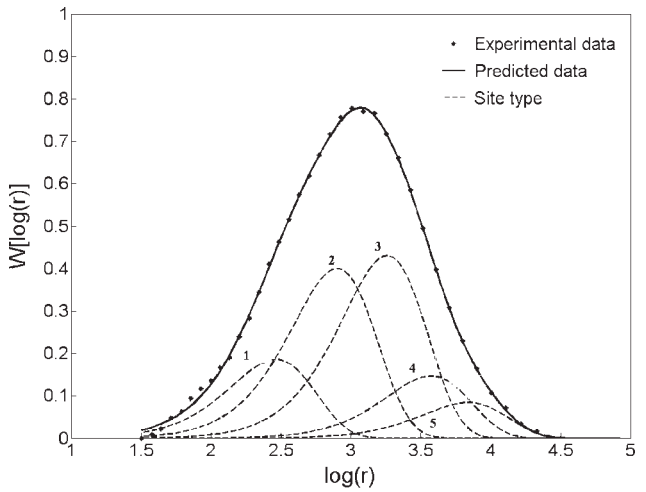

Figure 2 Resolution for GPC curves of PP produced by CS-1 catalyst. Experimental data at $T = 313$ K, Al/Ti = 98 (mol/mol), Si/Al = 0.05 (mol/mol), and $t = 2$ h. r represents the chain length, and w represents the most probable chain-length distributions.

possibilities are calculated using these constants and species' prompt concentrations. In a reaction time increment, random numbers determine the dynamic reaction following which the numbers of target species are modified. The next step is a statistical analysis of the molecule numbers and other characteristic quantities of the reaction mass. The simulation program should be executed in a loop with the newly calculated stochastic rate constants in terms of different temperatures or volumes until the truncation error meets a given criterion. However here, Monte Carlo simulation method is based on the basic theory of Gillespie with a few modifications due to the introduction of the five active sites for the CS-1 catalyst in this work. Accordingly, the modifications are also discussed by considering five active sites for the CS-1 catalyst.

For single active site Monte Carlo model for homogeneous propylene polymerization, the total number of the elementary reactions selected is four. Namely, eqs. (1)–(4). However, the total number of the elementary reactions selected for the polymerization catalyzed with the CS-1 catalyst is twenty, which differs from that for the polymerization catalyzed with single active site type catalyst. In addition, the classical Monte Carlo method just aims at one active "propagation" chain in the polymerization system, average MWD can be obtained by repeated simulation. However, for the five active site Monte Carlo simulation, the chain propagation, transfer and termination occuring on certain active site are selected randomly and restricted in certain given region according to corresponding chain concentration and rate constant. Therefore, to describe the broad MWD of the polymers, we must introduce the weight fraction of the active site which is constant during the polymerization. Furthermore, to avoid the "deficient" or "overplus" sampling problem that usually takes place when some reaction possibilities are extremely larger than others, a method of "bias sampling" is adopted in this work.[6]

The simulation of Monte Carlo in our study is programmed in C++ language. A series of pseudo-random numbers between 0 and 1 are generated by the starting point seeded by the CPU clock and with the help of another random number, the period of the generated number is prolonged. Considering the limitation of the computer, initial monomer molecule number is fixed at 1×10^9 and the monomer concentration is 1.0 mol/m^3, i.e. the total volume of the polymerization system, V, is about 1.66×10^{-15} m^3, the other parameters are analogically obtained. The reaction results including the changes of each active site type and the chain length of each site are recorded via the MSmodel. It lasts almost 8 hrs for the simulation of the reaction time up to 2 hrs on an Inter 2.13 GHz computer.

RESULTS AND DISCUSSION

Parameter estimation and model verification

To estimate the kinetic parameters, the values of the weight fractions of the active sites must be

TABLE I
Deconvolution Results of Two Representative Samples for Propylene Polymerization with the CS-1 Catalyst at Two Polymerization Times[a]

	Weight fraction (wt %)							
Site type	Sample 1 $t = 0.1$ hr	Sample 2 $t = 0.3$ hr	Sample 3 $t = 0.5$ hr	Sample 4 $t = 0.8$ hr	Sample 5 $t = 1$ hr	Sample 6 $t = 1.2$ hrs	Sample 7 $t = 1.6$ hrs	Sample 8 $t = 2$ hrs
1	9.49	8.94	9.07	7.54	10.60	13.08	13.29	14.88
2	18.40	19.35	18.74	19.48	18.60	17.58	28.22	27.10
3	39.13	41.00	42.18	41.59	40.67	43.47	34.09	36.51
4	23.74	23.76	21.95	23.19	22.50	16.80	15.40	14.77
5	7.03	6.95	8.06	8.20	7.63	9.07	9.00	6.74

[a] Polymerization conditions same as Figures 1 and 2.

TABLE II
Parameter Estimations for Propylene Polymerization with the CS-1 Catalyst[a]

Active site type (the jth type)	Weight fraction (wt %)	Kinetic constant (k)			
		$k_{i,j}$	$k_{p,j}$	$k_{trm,j}$	$k_{d,j} \times 10^5$
1	10.60	4279.97	4279.97	36.45	4.2
2	18.60	5268.77	5268.77	15.32	4.2
3	40.67	3996.04	3996.04	4.68	4.2
4	22.50	3996.04	3996.04	3.79	4.2
5	7.63	4278.89	4278.89	1.73	0.8

[a] Polymerization conditions same as Figures 1 and 2.

determined in advance. Table I lists these values. According to Figures 1 and 2 and Table I, one can know that the fraction of polymers produced from each active site type in Figures 1 and 2 (same system at 1 hr and 2 hrs) is quite different. In practice, we also find that the fraction of polymers produced from each active site type (here no data present), which is obtained via the deconvolution of MWD data, is different at different polymerization time. Furthermore, we find that the differences among the fractions in the early period of polymerization are obviously less than those in the anaphase of polymerization. As to the differences, one can understand that it is due to the cumulation of polymers with the polymerization proceeding. To test the above description, Table I lists typical data obtained by our experiment at under polymerization times. However, the cumulation of polymers can not alter the total number of the active site types of the CS-1 catalyst. Readers are encouraged to refer to Refs. 32, 33 to acquire more detailed information regarding this point. In practice, the above cumulation of polymers at different polymerization conditions (including polymerization time) can not be used to describe the instant polymerization kinetics over the Ziegler-Natta catalyst. Accordingly, the weight fraction data of the active sites obtained via the deconvolution of MWD data can not be used to reflect the multiple active sites of the catalyst. Therefore, the fraction of polymers produced from each active site type in the early period of polymerization should be used in the present work. Here the fraction data corresponding to 1 hr are used to the following estimation due to little difference of fraction data for each active site type before 1 hr or at 1 hr.

When the fraction data are determined, the estimations of the rate constants for each active site type can be made according to the experimental data. Corresponding MSmodel program builds a polymer yield–time curve with given rate constants and above weight fraction constants. The optimal rate constants are obtained through the comparison of the experimental and simulated data with an error expression that arrives a given minimum criterion,[7,11,25,31,34]

$$\text{Error } \% = \frac{1}{N}\sum\frac{|\text{Sim} - \text{Ind}|}{\text{Ind}}, \tag{7}$$

where Sim and Ind represent the simulated and experimental data respectively, and those data are the polymer yields at different polymerization time. N is the total number of the experimental data. The final constants adopted in this study are listed in Table II, and, corresponding comparison results are shown in Figure 3. Figure 3 illustrates the simulated data meet experimental data well and the optimal constant data shown in Table II can be used in the following study.

By using those constants shown in Table II, the MSmode can also provides average chain length including dead and active chain, polydispersity index and fraction of the total active site types, etc, for total active sites. In addition, polymerization rate, average chain length including dead and active chain, etc, for each active site, can be obtained via

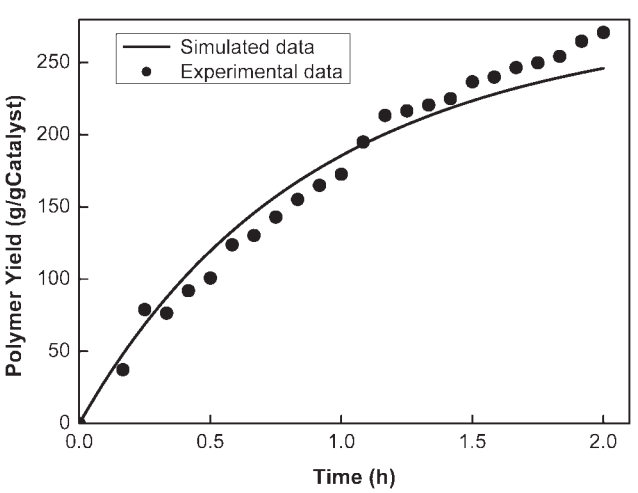

Figure 3 Comparison of the polymer yield-time curve of simulation and experiment. Simulated and experimental data at T = 313 K, Al/Ti = 98 (mol/mol), and Si/Al = 0.05 (mol/mol).

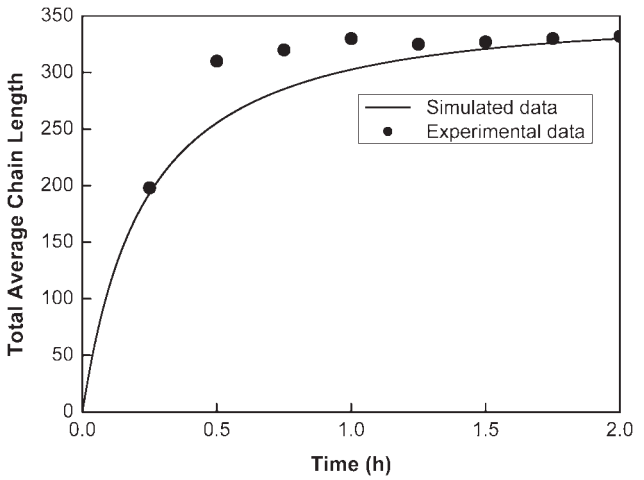

Figure 4 Comparison of the total average chain length-time curve of simulation and experiment. Simulated and experimental data at $T = 313$ K, Al/Ti = 98 (mol/mol), and Si/Al = 0.05 (mol/mol).

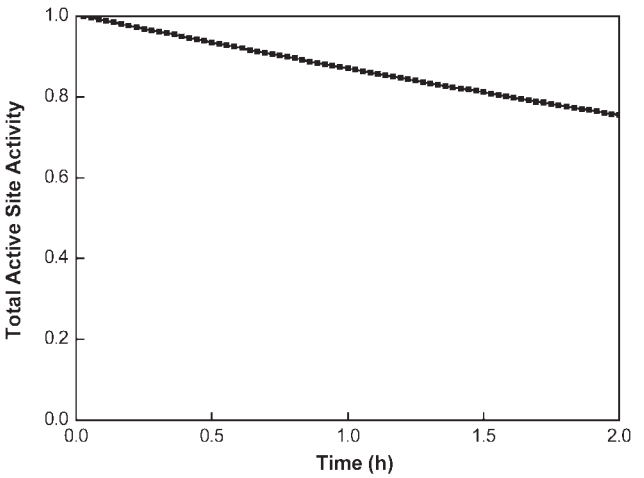

Figure 6 Simulated curve of the total polymerization activity of the active sites versus the time. Simulated and experimental data at $T = 313$ K, Al/Ti = 98 (mol/mol), and Si/Al = 0.05 (mol/mol).

the MSmodel. In this section, the curves of the average chain length and the polydispersity index versus the polymerization time for total active site types are obtained to examine the MSmodel.

Figure 4 shows that the comparison between the experimental average chain length and the simulated average chain length for total active site types during the propylene polymerization. Figure 5 shows the comparison of the polydispersity index during the propylene polymerization. According to Figures 4 and 5, one can know that the two groups of simulated data are slightly less than those from experiments. The above errors are mainly produced from the limited sampling and the constants of the weight fraction for each active site type throughout the polymerization used in our simulation. However, the compared results turn to be good as a whole. In conclusions, according to Figures 3–5, we can obtain that the simulated data agree well with the experimental data during the polymerization.

Polymerization kinetics over different active Sites

As the MSmodel is examined, it is used to simulate the polymerization kinetics for total active site types firstly. Figure 6 shows the simulated total active site activity in the polymerization process. It can be seen that the total active site activity seems to decrease at a beeline with the polymerization proceeding. Figure 7 illustrates the time-dependent total polymerization rate. From Figure 7, we can obtain that the total polymerization rate increases firstly in a short period

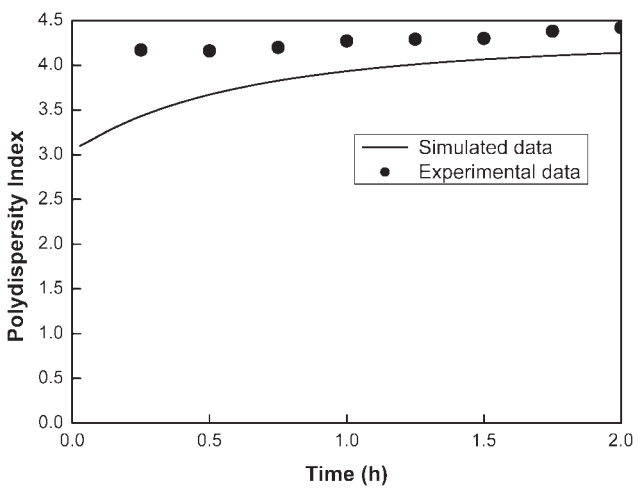

Figure 5 Comparison of the polydispersity index-time curve of simulation and experiment. Simulated and experimental data at $T = 313$ K, Al/Ti = 98 (mol/mol), and Si/Al = 0.05 (mol/mol).

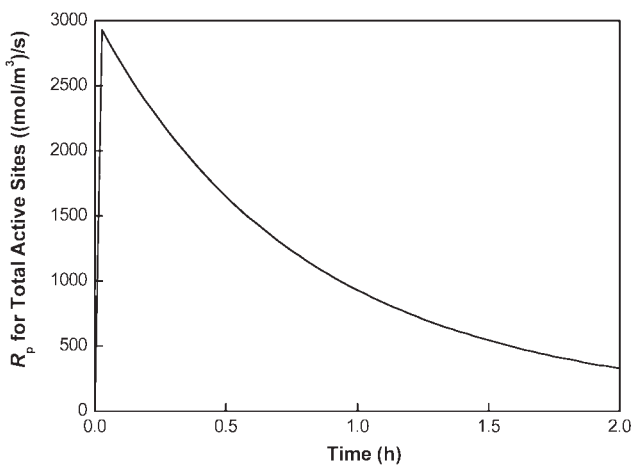

Figure 7 Simulated curve of the total polymerization rate of the active sites versus the time. Simulated and experimental data at $T = 313$ K, Al/Ti = 98 (mol/mol), and Si/Al = 0.05 (mol/mol).

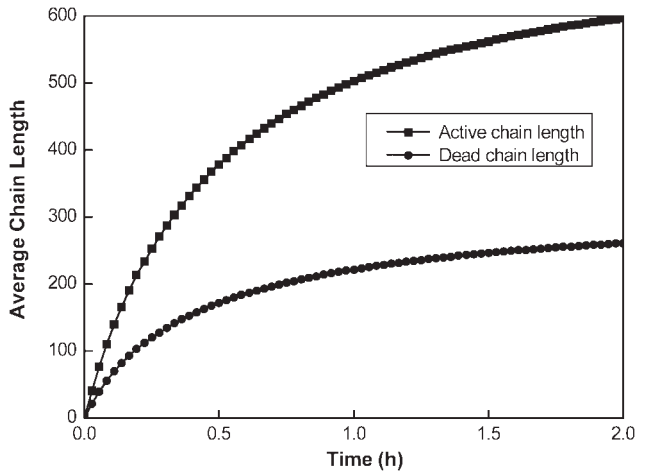

Figure 8 Simulated curve of the average chain length versus the time. Simulated and experimental data at T = 313 K, Al/Ti = 98 (mol/mol), and Si/Al = 0.05 (mol/mol).

and decreases quickly with the polymerization proceeding. In practice, the total polymerization rate can be written as:

$$R_p = \sum_{j=1}^{5} (k_{p,i}[C_j^*][M]), \quad (8)$$

where R_p represents the total polymerization rate, mol/(L s); j (j = 1,2,...,5) represents the type of the active site; $[C_j^*]$ represents the total active site concentration, mol/L; [M] represents the propylene concentration, mol/L. In the early period of the polymerization, [M] approaches to the top value, $k_{p,j}$ is a constant value at constant temperature, the polymerization rate increases quickly to its top value due to the quick increase of $[C_j^*]$ according to eq. (8). In the following polymerization, [M] and $[C_j^*]$ both decrease, which leads to the quick decrease of the total polymerization rate according to eq. (8). Figure 9 shows the time dependent the average chain length including the active chain length and the dead chain length. According to Figure 8, we can obtain that the simulated average active and dead chain lengths both increase with the polymerization proceeding in the period of 0–2 hrs. In addition, Figure 8 illustrates that the increase average rate of the active chain length increases faster than the dead chain length. Accordingly, we can conclude that the polymerization still continues and there are many monomers in the polymerization system at 2 h.

The simulated results above are obtained from the total active site type aspect. We can also simulate the polymerization kinetics for each active site type via the MSmodel. Figure 9 describes that the polymerization rate changes with the time for different active site types. According to Figure 9, we obtain that for each active site type, the polymerization rate decreases with the polymerization proceeding. In addition, the decrease speeds of the polymerization rates are different with each other for different active site types. As shown in Table II, among the active site types, the weight fraction of the third active site type is the maximal weight fraction, corresponding polymer yield and polymerization rate are also the maximum. For the second and fourth active site types, although the weight fraction of the fourth active site type is slightly higher than that of the second active site type, its chain-propagation rate constant value is 3996.04 and is less than that of the second active site type, namely 5268.77. Therefore, the polymerization rate of the second active site type is slightly higher than that of the fourth active site type according to eq. (8). Homoplastically, we also conclude that the polymerization rate of the first active site type is less than that of the fourth active site type and is higher than that of the fifth active site type. In practice, the above results can also be described in Figure 9. Figure 10 illustrates that the average dead chain length changes with the time for different active site types. For MSmodel, different average dead chain lengths corresponding to different active site types depend on the rate constants and reflect the broad MWD of the resulting polymers. In addition, the average dead chain length increases with the increase of the chain-propagation rate constant value and decreases with increase of the chain-transfer rate constant value.[2,35] Accordingly, the average dead chain length is determined by the joint effects of the two rate constant values.

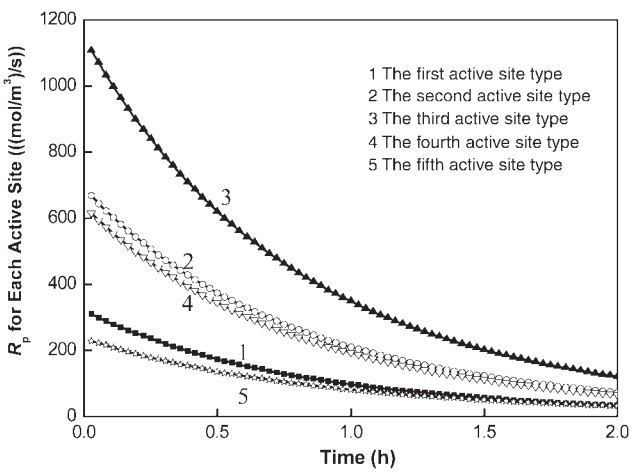

Figure 9 Simulated curve of the polymerization rate versus the time for each active site. Simulated and experimental data at T = 313 K, Al/Ti = 98 (mol/mol), and Si/Al = 0.05 (mol/mol).

Therefore, according to Table II and Figure 10, we can understand that the average dead chain length of the fifth active site type is the maximum, and the average dead chain length of the first active site type is the least. The average dead chain length of the third active site type is less than that of the fourth active site type but is higher than that of the second active site type. Figure 11 shows the average chain length distribution including active chain and dead chain at 2 hrs for total active site types and each active site type. Figure 11 proves that that multiple active site types result in a broad MWD when diffusion effect is ignored. In addition, Figure 11 illustrates the weight fraction of each active site type. Among them, the weight fraction of the third is the maximum, while the weight fraction of the fifth is the least. The weight fraction of the first one is higher than that of the fourth one but is less than that of the second one. In practice, the above results agree with that shown in Table II. Furthermore, combining Figure 2, it can be seen that the simulated data of MWD of polymers produced from the total active site types agree with those from the experiment at 2 h. However, it seems to be different between the simulated MWD data and those shown in Figure 2 of polymers produced from each active site type. As explained above, the difference is due to the constants of the weight fraction for each active site type throughout the polymerization used in our simulation, since these constants are determined based on the polymer sample at 1 h. Certainly, the above difference is small due to the small difference of fraction data for each active site in 1 hr and 2 hrs, respectively. Accordingly, it proves that the MWD values of polymers produced from the each active site and total active sits mainly depend on the fraction values for each active site type and corresponding kinetic constant values.

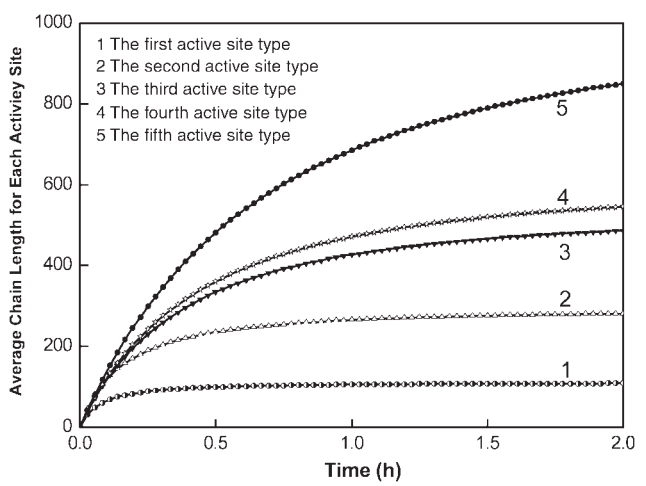

Figure 10 Simulated curve of the average chain length including active and dead chain versus the time for each active site. Simulated and experimental data at $T = 313$ K, Al/Ti = 98 (mol/mol), and Si/Al = 0.05 (mol/mol).

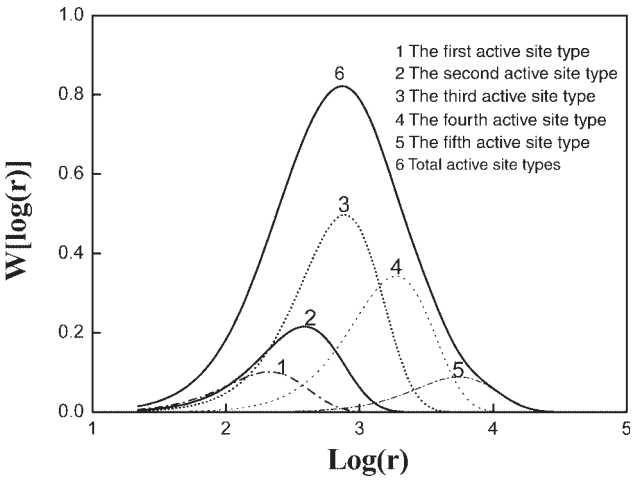

Figure 11 Modeling the chain length distribution including active and dead chain generated by a five-active-site-type catalyst. Simulated and experimental data at $T = 313$ K, Al/Ti = 98 (mol/mol), Si/Al = 0.05 (mol/mol), and $t = 2$ hrs. r represents the chain length, and w represents the most probable chain-length distributions.

CONCLUSIONS

A MSmodel is developed to describe the propylene polymerization kinetics catalyzed with the fourth heterogeneous Ziegler-Natta catalyst. Firstly, five active site types are present in the propylene polymerization based on an analysis of the GPC curves obtained via polymerization experiments. Secondly, Monte Carlo technique is used to simulate the propylene polymerization along with the multiple active sites. Good agreements in the polymerization kinetics are achieved for fitting the kinetic profiles with the MSmodel. In addition, the MSmodel is used to describe the dynamic evolution of the active sites and their effects on propylene polymerization.

The simulated results show that as the total active site activity decreases, the average active and dead chain lengths both increase yet with the polymerization proceeding. In addition, the total polymerization rate increases firstly in a short period and decreases quickly with the polymerization proceeding. Furthermore, the simulated results also show that for each active site type, the polymerization rate decreases following different rates and the dead chain length increases at different rate with the polymerization proceeding. In the mean time, the simulated result proves that multiple active site types result in a broad MWD.

The authors thank Dr. Chen Y. Z. (Department of Material Science and Engineering, Xiamen University) for his valuable discussion in this work. They also thank the anonymous referees for comments on this manuscript.

References

1. Zhan, X. L.; Luo, Z. H.; Chen, F. Q.; Yang, Y. R. Chem J Chin U 2003, 24, 1511 (in Chinese).
2. Soares, J. B. P. Chem Eng Sci 2001, 56, 4131.
3. Flory, P. J. J Am Chem Soc 1941, 63, 3083.
4. Platkowski, K.; Reichert, K. H. Polymer 1999, 40, 1057.
5. Tayakout-Fayolle, M.; Jallut, C.; Pollet, E. Chem Eng Sci 2003, 58, 1509.
6. He, J. P.; Zhang, H. D.; Chen, J. M.; Yang, Y. L. Macromolecules 1997, 30, 8010.
7. Soares, J. B. P.; Hamielec, A. E. Macromol React Eng 2008, 2, 115.
8. Mehdi, S. K.; Najafi, M.; Vahid, H. A.; Int., J. Chem Kinet 2009, 41, 45.
9. Mattos Neto, A. G.; Pinto, J. C. Chem Eng Sci 2001, 56, 4043.
10. Debling, J. A.; Han, G. C.; Kuijpers, F.; Verburg, J.; Zacca, J. J.; Ray, W. H. AIChE J 1994, 40, 506.
11. Luo, Z. H.; Zheng, Y.; Cao, Z. K.; Wen, S. H. Polym Eng Sci 2007, 47, 1643.
12. Luo, Z. H.; Zheng, Y.; Cao, Z. K.; Wen, S. H.; Chinese, J. Polym Sci 2007, 25, 365.
13. Mckenna, T. F.; Dupuy, J.; Spitz, R. J Appl Polym Sci 1995, 57, 371.
14. Mckenna, T. F.; Dupuy, J.; Spitz, R. J Appl Polym Sci 1997, 63, 315.
15. Shaffer, W. K. A.; Ray, W. H. J Appl Polym Sci 1997, 65, 1053.
16. Mckenna, T. F.; Soares, J. B. P. Chem Eng Sci 2001, 56, 3931.
17. Luo, Z. H.; Cao, Z. K.; Su, Y. T.; Chinese, J. Chem Eng 2006, 14, 194.
18. Luo, Z. H.; Wang, W.; Su, P. L. J Appl Polym Sci 2008, 110, 3360.
19. Simon, L. C.; Soares, J. B. P. Ind Eng Chem Res 2005, 44, 2461.
20. Simon, L. C.; Williams, C. P.; Soares, J. B. P. Chem Eng Sci 2001, 56, 4181.
21. Soares, J. B. P.; Hamielec, A. E. Polymer 1995, 36, 2257.
22. Soares, J. B. P.; Kim, J. D.; Rempel, G. L. Ind Eng Chem Res 1997, 36, 1144.
23. Chien, J. C. W. J Polym Sci 1979, 17, 2555.
24. Zhu, Y. M.Sc thesis, Xiamen University, Xiamen, 2008 (in Chinese).
25. Wang, J.; Luo, Z. H.; Zhu, Y. Chem Eng (China) 2009, 37, 41 (in Chinese).
26. Floyd, S.; Choi, K. Y.; Taylor, T. W.; Ray, W. H. J Appl Polym Sci 1986, 31, 2231.
27. Floyd, S.; Choi, K. Y.; Taylor, T. W.; Ray, W. H. J Appl Polym Sci 1986, 32, 2935.
28. Zacca, J. J.; Ray, W. H. Chem Eng Sec 1993, 48, 3743.
29. Kissin, Y. V. J Polym Sci Polym Chem 1995, 33, 227.
30. Gillespie, D. T. J Phys Chem 1977, 81, 2340.
31. Ling, J.; Ni, X. F.; Zhang, Y. F.; Shen, Z. Q. Polymer 2000, 41, 8703.
32. Luo, Z. H.; Su, P. L.; Shi, D. P.; Zheng, Z. W. Chem Eng J 2009, 149, 370.
33. Su, P. L. M.Sc thesis, Xiamen University, 2009 (In Chinese).
34. Ling, J.; Zhang, Y. F.; Shen, Z. Q.; Jie, N. Eur Polym J 2001, 37, 2407.
35. Wang, Q.; Weng, J. H.; Xu, L.; Fan, Z. Q.; Feng, L. X. Polymer 1999, 40, 1863.